water

MDPI

Article

EMD-RBFNN Coupling Prediction Model of Complex Regional Groundwater Depth Series: A Case Study of the Jiansanjiang Administration of Heilongjiang Land Reclamation in China

Qiang Fu [1,2,3], Dong Liu [1,2,3,*], Tianxiao Li [1], Song Cui [1] and Yuxiang Hu [1]

1 School of Water Conservancy & Civil Engineering, Northeast Agricultural University, Harbin 150030, China; fuqiang0629@126.com (Q.F.); litianxiao@neau.edu.cn (T.L.); cuisong-bq@neau.edu.cn (S.C.); huyuxiang2003@163.com (Y.H.)

2 Heilongjiang Provincial Collaborative Innovation Center of Grain Production Capacity Improvement, Northeast Agricultural University, Harbin 150030, China

3 Key Laboratory of High Efficient Utilization of Agricultural Water Resource of Ministry of Agriculture, Northeast Agricultural University, Harbin 150030, China

* Correspondence: liu72dong@126.com; Tel.: +86-451-55191501

Academic Editor: Y. Jun Xu

Received: 29 June 2016; Accepted: 4 August 2016; Published: 10 August 2016

Abstract: The accurate and reliable prediction of groundwater depth is the basis of the sustainable utilization of regional groundwater resources. However, the complexity of the prediction has been ignored in previous studies of regional groundwater depth system analysis and prediction, making it difficult to realize the scientific management of groundwater resources. To address this defect, taking complexity diagnosis as the research foundation, this paper proposes a new coupling forecast strategy for evaluating groundwater depth based on empirical mode decomposition (EMD) and a radial basis function neural network (RBFNN). The data used for complexity analysis and modelling are the monthly groundwater depth series monitoring data from 15 long-term monitoring wells from 1997 to 2007, which were collected from the Jiansanjiang Administration of Heilongjiang Agricultural Reclamation in China. The calculation results of the comprehensive complexity index for each groundwater depth series obtained are based on wavelet theory, fractal theory, and the approximate entropy method. The monthly groundwater depth sequence of District 8 of Farm Nongjiang, which has the highest complexity among the five farms in the Jiansanjiang Administration midland, was chosen as the modelling sample series. The groundwater depth series of District 8 of Farm Nongjiang was separated into five intrinsic mode function (IMF) sequences and a remainder sequence by applying the EMD method, which revealed that local groundwater depth has a significant one-year periodic character and an increasing trend. The RBFNN was then used to forecast and stack each EMD separation sequence. The results suggest that the future groundwater depth will remain at approximately 10 m if the past pattern of water use continues, exceeding the ideal depth of groundwater. Thus, local departments should take appropriate countermeasures to conserve groundwater resources effectively.

Keywords: Jiansanjiang administration; groundwater depth; complexity; empirical mode decomposition; radial basis function neural network

1. Introduction

Groundwater is an important foundational resource to support sustainable regional social and economic development. With the rapid development of the population and economy, the imbalance

between the supply and demand of groundwater resources has become increasingly prominent, becoming the main limiting factor of regional agricultural development. Driven by high-intensity agricultural development, the regional complexity of the groundwater resource system is becoming increasingly prominent [1], evoking many ecological environmental problems such as decreasing groundwater depth and deteriorating water quality. Groundwater depth is an important system element of the groundwater resource system. Predicting groundwater depth accurately is the basis for using and managing groundwater resources effectively. Generally, we have built prediction models under the guidance of the average groundwater monitoring data of certain monitoring stations or regions. The conventional prediction method ignores the complexity of information related to the changing patterns of groundwater depth, resulting in useless prediction results. Against this background, it is becoming increasingly urgent in the field of hydrology to clarify the complex information related to regional groundwater depth and analyse the changes in groundwater depth.

Groundwater depth series analysis and prediction are prerequisites for managing regional groundwater resources. Generally, the higher the complexity of a groundwater depth sequence, the lower its predictability [2,3]. Thus, for a highly complex groundwater depth sequence, we should pay more attention to choosing a suitable method for improving prediction. There are many groundwater depth prediction methods, such as the artificial neural network model, artificial neural network and wavelet analysis, adaptive neuro-fuzzy inference system, self-organizing maps, genetic algorithm, other coupling models, autoregressive moving average exogenous (ARMAX) based on the aquifer dynamic model, hydrology continuity equation, "panel-data" model, Markovian stochastic model and automatic parameter calibration SCE method [4–13]. These methods have limitations when applied in non-stationary time series; some ignore the complexity of the problem, some result in poor extension, and some have complex principles that result in inaccurate predictions.

In 1998, Huang et al. [14] proposed a new method of nonlinear, non-stationary time series analysis empirical mode decomposition (EMD). The EMD method possesses a self-adaptive characteristic, overcomes the difficulty in choosing a basis function and other questions in wavelet analysis, and has stronger local performance ability than wavelet analysis. EMD is a very effective data mining tool that can break the original data into a series of components of intrinsic mode functions (IMFs), and it possesses local feature information based on different time scales and obvious physical backgrounds. At the same time, EMD can analyse trends in data sequences [15]. Therefore, the EMD method has been widely used in different fields such as finance, astronomy, fault diagnosis and medical science and has achieved satisfactory results. Guhathakurta [16] adopted the EMD method to analyse and compare the daily dynamics of the NIFTY index in India's national stock exchange with the ALL Ordinary Index (AOI) of the Hong Kong stock exchange. He also divided the geopotential height of the Northern Hemisphere into one trend and five IMF components, including period, standard two-year period oscillation, similar El Niño periods, and the 11-year sun activity cycle [17]. Bassiuny et al. [18] combined the EMD method and learning vector quantization (LVQ) network method, extracted the main characteristic of the strain signal in the process of metal flake stamping and classified the faults in the stamping process. They also used the EMD method to eliminate the high-frequency noise and baseline drift in electrocardiogram (ECG) signals [15].

Hydrological time series usually appear as smooth, nonlinear signals. Some scholars have attempted to use EMD to perform hydrological time series forecast analysis. Sinclair focused on the implementation and development of the two-dimensional extension to the EMD algorithm and its application to radar rainfall data of Bethlehem in South Africa and the examination of temporal persistence in the data in different spatial situations [19]. Iyengar and Raghu [20] decomposed monsoon rainfall data into six IMF components based on eight regions' rainfall data in India using the EMD method. They then applied the artificial neural network and linear regression techniques to address the nonlinear first IMF component and the other IMF components, respectively; stacked the reduction; and ultimately forecast monsoon rainfall in India [20]. Huang et al. [21] presented a fluctuation characteristics analysis of the daily river flow data from the Seine river (France) and Wimereux River

(Wimereux, France) using the EMD method and described the intermittent fluctuations of the Seine River with arbitrary-order Hilbert spectral analysis. McMahon et al. [22] adopted the EMD method to extract the low-frequency characteristics of the annual runoff series of 595 rivers across the world. The variance of the low-frequency wave ratio was calculated. At present, however, the EMD method is mainly used for precipitation, runoff sequence analysis and forecasting in the water resources field and is less often used for groundwater depth sequence analysis and prediction.

The EMD method can break the groundwater depth data into a series of components of IMF with different physical meanings. However, it still requires some auxiliary methods to predict groundwater depth. The artificial neural network is an effective tool for time series prediction and has nonlinear approximation ability. Among such methods, the backpropagation neural network (BPNN) has been commonly used. However, there are many problems with BPNN; for example, it is not easy to produce a local optimal solution, slow down the convergence speed, and reduce the difficulties in determining the network structure [23,24]. In contrast, the radial basis function neural network (RBFNN) can overcome the deficiencies of the BPNN with a faster convergence rate, fewer extrapolation errors, simpler topological structure and higher reliability and other advantages. RBFNN has been widely used in hydrological time series prediction [6,7].

The goal of this paper is to establish a groundwater depth coupling forecast model of the Jiansanjiang Administration midland of Heilongjiang Agricultural Reclamation in China combined with the EMD RBFNN method and the complexity measure theory, selecting the most complex groundwater depth sequence as the sample series.

The remainder of the paper is organized as follows. Section 2 briefly introduces the general information on the study area and describes the basic data used in this study. The methods employed in this study are presented in Section 3. Section 4 presents and discusses the results obtained from real groundwater depth series data. Finally, conclusions are given in Section 5.

2. Study Area and Data Description

2.1. Study Area

Jiansanjiang Administration is on the Sanjiang Plain in Heilongjiang Province of China and is at the junction of two towns (Fujin and Tongjiang) and two counties (Fuyuan and Raohe). This area is located in northeastern China and stretches between 46°49′42″ N–48°13′58″ N and 132°31′26″ E–134°22′26″ E, with a total land area of 12,300 km^2 and a cultivated area of 682,000 hm^2; 15 large and medium-sized state-owned farms (Figure 1) are included. Jiansanjiang Administration is a suitable place for rice planting and is the green rice production centre in China [25]. The middle district of Jiansanjiang Administration includes farms of Qianjin, Honghe, Qianfeng, Erdaohe and Qianshao, with a total land area of 3747.85 km^2. In 2009, the agricultural coverage was 240,000 hm^2. The district contains the national nature reserve of Honghe and the provincial nature reserve of Qianfeng, which mainly include cultivated rice, maize, soybeans and wheat with higher mechanization and commodity grains. Since the 1990s, the district has been planted in rice and the acreage has increased annually; by 2009, it was 16.3×10^4 hm^2, taking up 67.9% of the total agricultural acreage. However, because of the lack of a control project, inefficiency of surface water utilization, and dependence of agricultural irrigation on groundwater, the complex features of Jiansanjiang Administration are becoming increasingly obvious, resulting in a continuous decline of the groundwater level. Meanwhile, the influence of climate conditions (precipitation, evaporation, and temperature), hydrogeological conditions (supply conditions) and other natural factors leading to complex characteristics such as nonlinearity and randomness of groundwater depth is important. Therefore, it is necessary to study the complexity of groundwater depth series in the Jiansanjiang Administration midland to analyse the groundwater depth development trend and provide basic guidance for the regional management of groundwater resources.

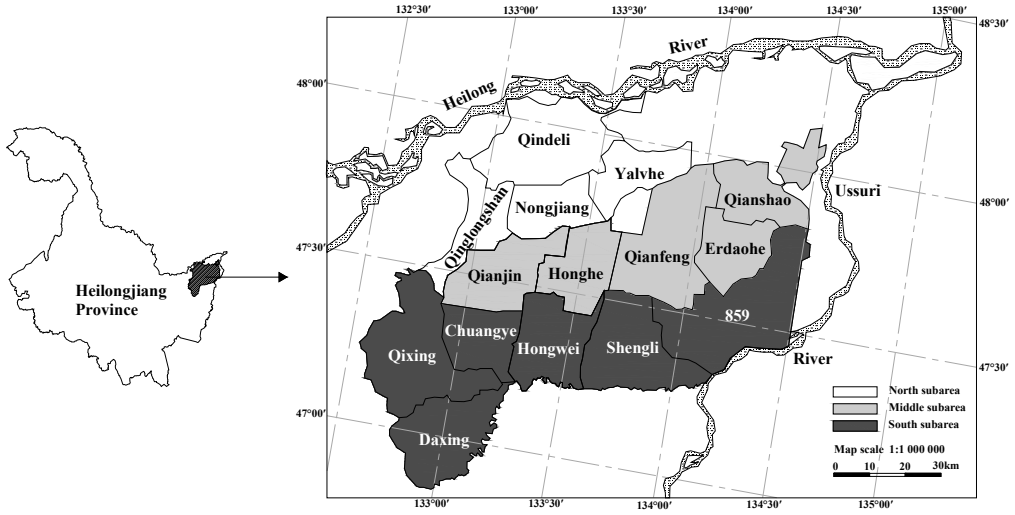

Figure 1. Location of Jiansanjiang Administration in Heilongjiang Province.

2.2. Data Description

The long-term monthly groundwater depth series monitoring data from 15 farms from 1997 to 2007 were collected from the Water Affairs Administration of Jiansanjiang Land Reclamation Administration of Heilongjiang Province. The variation curves (Figure 2) of groundwater depth series H_t (t = 1, 2, . . . , 132) of each farm take the data of every monitoring point as that of each district. The average amplitude of each monthly groundwater depth series was calculated (Table 1).

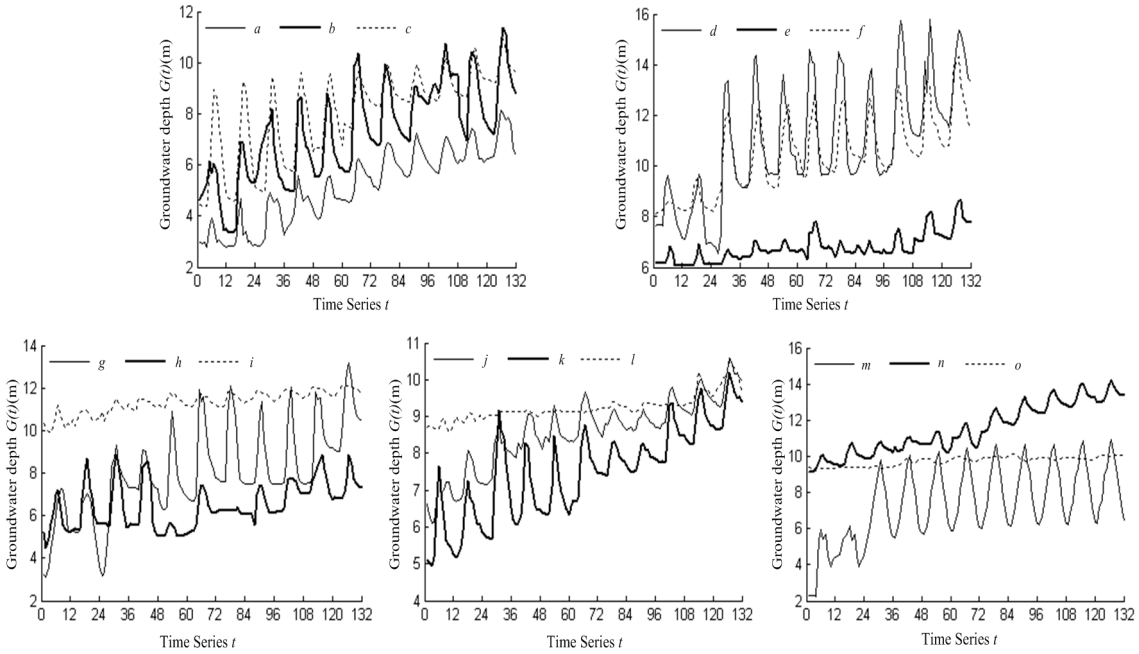

a. Subarea 1 of Farm 859; *b*. Subarea 69 of Farm Qixing; *c*. Subarea 22 of Farm Qianjin; *d*. Subarea 24 of Farm Chuangye; *e*. District 5 of Farm Yalvhe; *f*. Subarea 28 of Farm Hongwei; *g*. District 8 of Farm Nongjiang; *h*. Subarea 17 of Farm Qinglongshan; *i*. Subarea 36 of Farm Qindeli; *j*. Ministry of Farm Qianfeng; *k*. District 6 of Farm Honghe; *l*. District 5 of Farm Erdaohe; *m*. Subarea 11 of Farm Daxing; *n*. Subarea 31 of Farm Shengli; *o*. 12th production team of Farm Qianjin

Figure 2. Variation Curve of Monthly Groundwater Depth Series of Each Farm in Jiansanjiang Administration from 1997 to 2007.

Table 1. Annual Average Monthly Change of Groundwater Depth Series of Each Farm in Jiansanjiang Administration of China.

The Location of Long-Term Monitoring Wells	The Number of Long-Term Monitoring Wells	Average Groundwater Depth (m)		Annual Average Increase (m)
		1997	2007	
Subarea 1 of Farm 859	01	3.12	7.14	0.40
Subarea 69 of Farm Qixing	02	4.92	9.15	0.42
Subarea 22 of Farm Qianjin	03	6.09	9.81	0.37
Subarea 24 of Farm Chuangye	04	8.14	13.47	0.53
District 5 of Farm Yalvhe	05	6.26	7.77	0.15
Subarea 28 of Farm Hongwei	06	8.35	12.34	0.40
District 8 of Farm Nongjiang	07	5.31	10.84	0.55
Subarea 17 of Farm Qinglongshan	08	5.69	7.44	0.18
Subarea 36 of Farm Qindeli	09	10.35	11.90	0.16
Ministry of Farm Qianfeng	10	6.80	9.91	0.31
District 6 of Farm Honghe	11	5.81	9.34	0.35
District 5 of Farm Erdaohe	12	8.73	10.04	0.13
Subarea 11 of Farm Daxing	13	4.06	8.51	0.45
Subarea 31 of Farm Shengli	14	9.55	13.47	0.39
Subarea 12 of Farm Qianshao	15	9.35	10.03	0.07

It can be seen in Figure 2 that the monitoring groundwater depth obviously increased under the influence of several factors, especially in high-intensity agricultural production activities. Each groundwater depth series has obvious cyclical characteristics, but they belong to the non-stationary time series, and the dynamic changes also involve other complex characteristics, including randomness and nonlinearity, because the mean and variance changes are not smooth. Table 1 shows that from 1997 to 2007, the annual average growth of the groundwater depth of 5 farms, including Yalvhe, Qinglongshan, Qindeli, Qianshao and Erdaohe, was less than 0.2 m, which is not particularly high. However, the annual average increase of the other 10 farms was greater than 0.3 m, which suggests that a local agricultural irrigation pattern that depends on groundwater has a direct influence on the dynamic change of the groundwater level. Among the five farms located in the central Jiansanjiang Administration, the increase in annual average groundwater depth of Erdaohe and Qianshao is small; the others are larger. The average annual groundwater depth of these five farms is 0.25 m. In addition, the monthly groundwater depth series of the five central farms has an obvious complex change dynamic between years and inter-annual fluctuations, except for Erdaohe and Qianshao. The complexity measure of the monthly groundwater depth sequence still must be recognized, which can help choose which sequence can be set as a representative sample to analyse the complex evolution of central groundwater depth in Jiansanjiang Administration.

3. Methods

3.1. The Diagnosis Method of the Complexity of Hydrological Series

There are some commonly used complexity measurement methods of hydrological series, including wavelet entropy (*WE*) [26], approximate entropy (*ApEn*) [27], Lempel–Ziv complexity (*LZC*) [28], resealed range analysis (R/S analysis) [29], discrete wavelet transform (*DWT*) fractal theory [30], continuous wavelet transform (*CWT*) fractal theory [31], and others, and the specific algorithm can be referenced.

3.2. EMD

3.2.1. Basic Concepts

If the difference between the maximum (or minimum) number in some time series $f(t)$ and the zero-up-crossing (or zero-down-crossing) number is equal to or greater than two, the sequence must

be smoothed, which will generate a series of IMF components. IMF should satisfy the following two conditions [14]:

(1) In the total data range, the number of extreme value points is equal to or no greater than one different from the number of zero-crossing points;
(2) At any point, the average value of upper and lower limits made by the maximum points and minimum points, which are equal to zero.

3.2.2. Concrete Steps

The concrete steps of using the EMD method to work with a time series $f(t)$ are as follows [14–16,18,19,21]:

(1) Determine all maximum and minimum points in a sequence $f(t)$, and then fit them into the up envelope $e_a(t)$ and down envelope $e_b(t)$ of the sequence $f(t)$, respectively, with the cubic spline function.
(2) Calculate the mean value $m_1(t)$ of the up and down envelopes

$$m_1(t) = [e_a(t) + e_b(t)]/2 \tag{1}$$

(3) Calculate the interpolating sequence $h_1(t)$

$$h_1(t) = f(t) - m_1(t) \tag{2}$$

Generally, $h_1(t)$ cannot satisfy the IMF conditions.

(4) Take $h_1(t)$ as a new sequence, repeat steps (1) to (3), and apply k iterations of screening to $h_1(t)$; namely,

$$(t) = h_{1k}(t). \tag{3}$$

In practical operation, the limited standard deviation (SD) is used as the stopping rule in the screening process:

$$SD = \sum_{t=1}^{N} \frac{\left| h_{1(k-1)}(t) - h_{1k}(t) \right|^2}{h_{1(k-1)}^2(t)} \tag{4}$$

where N is the number of sample sequences.

If after k iterations of screening, $h_{1k}(t)$ satisfies the result 0.2 < SD < 0.3, the first IMF component, IMF1(t) = $h_{1k}(t)$, is obtained.

(5) Calculate the remaining sequence $r_1(t)$

$$r_1(t) = f(t) - \mathrm{IMF1}(t) \tag{5}$$

(6) Take $r_1(t)$ as the new sequence to be decomposed, and repeat steps (1) to (5), resulting in

$$\begin{cases} r_2(t) = r_1(t) - \mathrm{IMF2}(t) \\ r_3(t) = r_2(t) - \mathrm{IMF3}(t) \\ \quad \vdots \quad \vdots \quad \vdots \\ r_n(t) = r_{n-1}(t) - \mathrm{IMF}n(t) \end{cases} \tag{6}$$

until the information contained in the remaining sequence $r_n(t)$ is of little significance to study or has become a monotonic function that is unable to screen out IMF. At that time, the remaining $r_n(t)$ represents the average trend of the original sequence, which is called the remainder or trend

term. The original sequence can be expressed by a sum of a series of IMF components and trend terms, namely,

$$f(t) = \sum_{i=1}^{n} \mathrm{IMF}i(t) + r_n(t) \tag{7}$$

3.2.3. End Effect

There is no way to determine whether the ends are equal to the extreme value points in the course of applying the EMD method. If we regard the end of the sequence as the extreme value point directly, there will be divergence; the upper and lower envelopes will deviate from the original sequence's real envelope near the series endpoint when using three-spline interpolation, and along with the continuing "screening process", this expansion result will "pollute" the whole data sequence gradually, leading to incorrect results. This effect deprives the actual physical significance of IMF, which is called the end effect [14,17,18,32,33]. To improve the EMD method application effect, we must adopt the appropriate method for the sequence continuations and abandon the "pollution" points, thus restraining the existing boundary effect [4,34]. Many scholars have studied the end effect problems of the EMD and proposed various methods, including regression models, the technique of artificial neural networks, the mirror method, the improved slope method [32], the SZero method (three-spline curve slope is zero at the ends) [33], the variable cosine window method [35], and the oblique-extreme method [36]. This paper attempts to use RBFNN to solve the EMD method end effect.

3.3. Radial Basis Function Neural Network

3.3.1. The Network Structure

An RBFNN is composed of three layers: an input layer, a hidden layer and an output layer. The hidden layer consists of a set of basis functions performing nonlinear transformations of the inputs. The most common transformation is the Gaussian function as the nonlinearity of the hidden nodes, whereas the output layer is linear [6,7,23,24].

3.3.2. Basic Concepts

Take the radial basis function as the "base" of the hidden layer and map the input vector to the hidden layer space directly but not through the right connections. When the centre of the radial basis function is determined, the nonlinear mapping relation is also determined. The relationship between the hidden layer space and the output layer is linear mapping; thus, the network output is the linear weighted a sum of hidden layer output [6,7,23,24,37,38].

3.4. EMD-RBFNN Coupling Forecast Model

First, continue to combine data with RBFNN to obtain the IMF component and trend term of the hydrological time series with the EMD method. Then, predict each IMF component and trend term obtained from the RBFNN decomposition. Finally, superpose each IMF component and the predicted trend term values to obtain the original sequence predictive values. This model is called the EMD-RBFNN coupling model based on the above concepts, and the specific structure is shown in Figure 3.

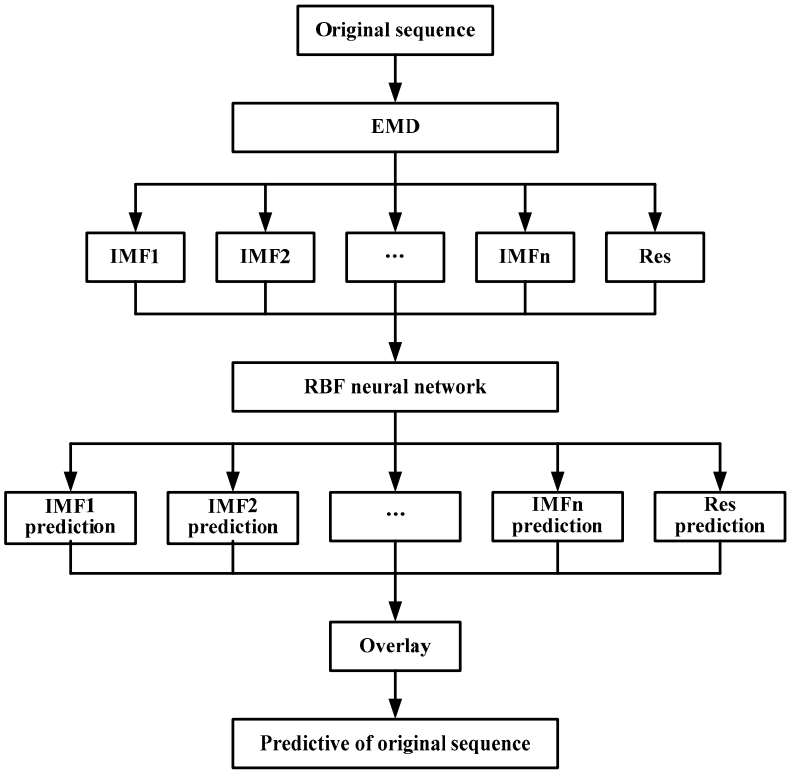

Figure 3. Flow path of EMD-RBFNN coupling model.

4. Results and Discussion

4.1. The Complexity Measure of the Groundwater Depth Sequence

To fully consider the mutual influence of the groundwater depth's complex dynamic changes on each farm, we adopted the above six methods to measure the monthly groundwater depth sequence complexity in Jiansanjiang Administration. The sorted results are shown in Table 2 (the results for only the 5 central farms are shown). Among the above complexity measurement methods, the rescaled range analysis fractal theory is more sensitive to the sequence's length, which is of biased estimation and poor stability [39]. The stability of the continuous wavelet transform fractal theory [31] is higher, and the other methods are of mid-degree stability. To take full advantage of every complexity measurement method, this thesis determined the weight of each complexity measure w_i (i = 1, 2, . . . , 6) according to the above analysis, as shown in Table 2.

Table 2. Comprehensive Complexity Index Calculation of Monthly Groundwater Depth Series of Each Farm in Jiansanjiang Administration of China.

Location of the Long-Term Monitoring Well	*WE* (0.16)		*ApEn* (0.16)		*LZC* (0.16)		*D*						C_{Ij}	Complexity Sort
							R/S Analysis Method (0.12)		Wavelet Estimator Method					
									DWT (0.16)		*CWT* (0.24)			
	sort	value	sort	value	sort	value	sort	value	sort	value	sort	value		
Subarea 22 of Farm Qianjin	⑭	2	③	13	⑧	8	⑦	9	⑧	8	⑤	11	8.68	⑥
District 6 of Farm Honghe	⑥	10	④	12	④	12	⑨	7	⑦	9	⑧	8	9.64	③
Ministry of Farm Qianfeng	②	14	⑥	10	⑫	4	③	13	③	13	⑪	5	9.32	④
District 5 of Farm Erdaohe	⑪	5	⑮	1	⑮	1	⑧	8	⑫	4	⑬	3	3.44	⑮
Subarea 12 of Farm Qianshao	①	15	⑬	3	⑩	6	⑩	6	⑨	7	⑭	2	6.16	⑬

Notes: ① The values in brackets are the methods' weights of groundwater depth series complexity; ② D is the fractal dimension.

By attaching the corresponding score S_i = 15–1 to monthly groundwater depth sequence complexity sort results (①–⑮) in Jiansanjiang Administration, we can obtain the groundwater depth sequence's comprehensive complexity index calculation formula:

$$C_{Ij} = \sum_{i=1}^{6} s_i w_i \tag{8}$$

where C_{Ij} is the jth comprehensive complexity index of the groundwater depth sequence, j = 1, 2, ..., 15.

According to Equation (8) used to calculate the monthly groundwater depth sequence comprehensive complexity index in Jiansanjiang Administration, the results are shown in Table 2 (the results for only the 5 central farms are shown). Table 2 shows that the comprehensive complexity sorting of monthly groundwater depth of Jiansanjiang Administration is as follows: District 6 of Farm Honghe > Ministry of Farm Qianfeng > Subarea 22 of Farm Qianjin > Subarea 12 of Farm Qianshao > District 5 of Farm Erdaohe. Among the five central groundwater depth monitoring stations, the C_{Ij} value of District 6 of Farm Honghe is the highest, which suggests that there are many regional groundwater depth impact factors, and the complexity of the relative groundwater system dynamics structure is the strongest.

4.2. EMD-RBFNN Coupling Predictive Model of Groundwater Depth

The above calculation analysis shows that the groundwater depth complexity of District 6 of Farm Honghe is the highest among the five central monitoring stations and can best reflect all types of complicated factors that influence the regional groundwater depth dynamic change. Therefore, this thesis selected the monthly groundwater depth sequence of District 6 of Farm Honghe as a representative sample and took the analysis results of dynamic change regulation as the general characteristics of groundwater depth dynamic change in central Jiansanjiang Administration. We now establish the EMD-RBFNN coupling forecasting model according to the monthly groundwater depth sequence data of District 6 of Farm Honghe from 1997 to 2006 (Figure 4) and take the monthly groundwater depth sequence data of 2007 as a reserved inspection.

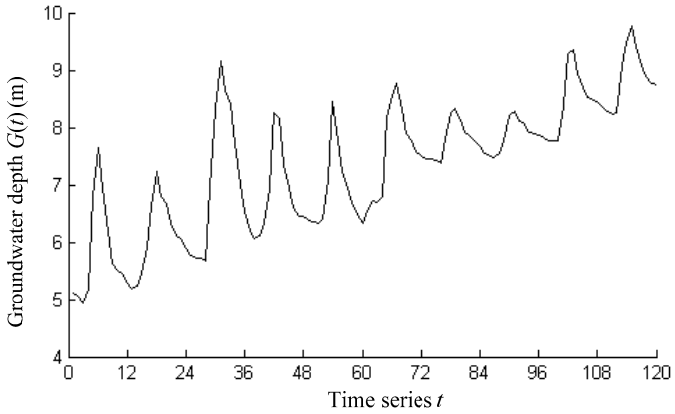

Figure 4. The Monthly Groundwater Depth Series Variation Curve of District 6 of Farm Honghe (1997–2006).

4.2.1. Empirical Mode Decomposition of Monthly Groundwater Depth Sequence

Decompose the monthly groundwater depth sequence $G(t)$ (t = 1–120) of District 6 of Farm Honghe with the EMD method described above and adopt the RBFNN for boundary extension, set the RBFNN target error GOAL = 0.0001, spread constant SPREAD = 1.5, and number of maximum neurons MN = 30. Through the program calculation, five output IMF components and a remainder of sequence $G(t)$ are generated; see Figure 5.

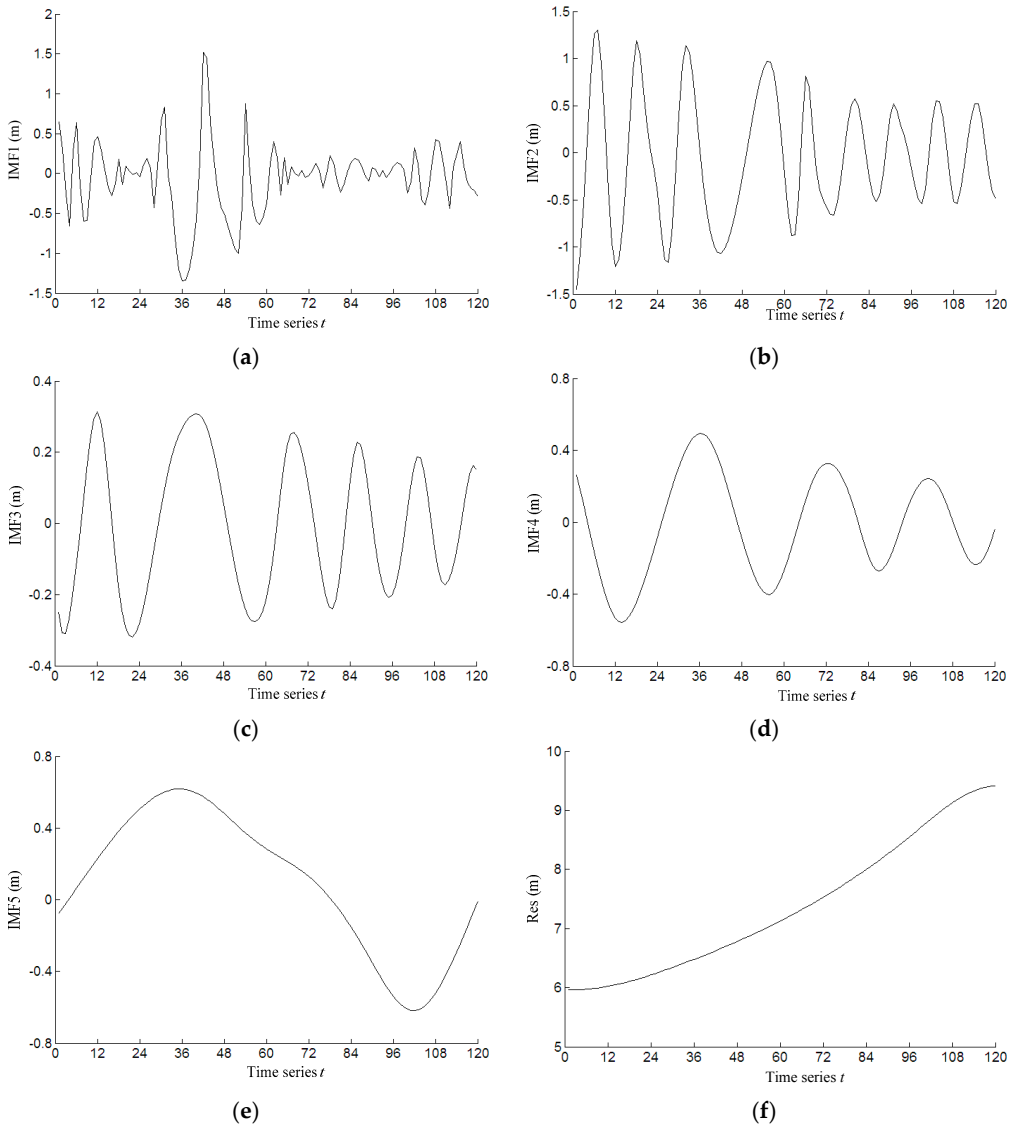

Figure 5. The IMF Component and Trend Term of Monthly Groundwater Depth Series in District 6 of Farm Honghe.

In Figure 5, IMF1 stands for the high-frequency component whose period is less than one year with a main circulation cycle less than 0.5 years. This means that the groundwater depth can respond to agricultural production activities (groundwater development), and the main amplitude of groundwater depth is approximately 0.1–0.5 m, accompanied by large-amplitude fluctuation of approximately 0.8–1.5 m; IMF2, whose amplitude is approximately 0.5–1.2 m, indicates the significant concussion cycle for one year and represents the recharge response of the groundwater depth to the precipitation or other groundwater; IMF3, whose amplitude is approximately 0.2–0.3 m, has obvious periodic oscillation of 1.5–2.5 m and represents the response of the groundwater depth to 1.5–2.5 years of annual precipitation; IMF4, whose amplitude is approximately 0.2–0.5 m and whose cycle is approximately 3 years, represents the groundwater depth response to 3 years of annual precipitation; IMF5, whose amplitude is approximately 0.6 m and whose cycle is approximately 12 years, represents the groundwater depth response to 12 years of annual precipitation; Res represents the overall trend of the groundwater depth.

The variance contributions of each IMF component and trend term are shown in Table 3. Table 3 shows that the variance contribution rate of Res is the largest, which reached 58.25%; this increase

results in the consistent overall increasing trend of the groundwater depth sequence of District 6 of Farm Honghe. Among each IMF component's variance contribution rate, IMF2 had the largest, reaching 19.45%, and carried the most information [40], which suggests that the local groundwater depth undergoes dynamic changes and a main cycle of one year.

Table 3. EMD Component Variance Contribution Rate of the Monthly Groundwater Depth Series in District 6 of Farm Honghe.

EMD Component	IMF1	IMF2	IMF3	IMF4	IMF5	Res
Variance contribution rate (%)	9.83	19.45	1.72	3.66	7.09	58.25

4.2.2. Monthly Groundwater Depth Prediction

Determinate Input and Output Samples

Because sequence $G(t)$ produces five IMF components and one remainder term through empirical mode decomposition, it must structure six RBFNNs. Combined with the former analysis, the monthly groundwater depth dynamic change regulation of District 6 of Farm Honghe exhibits an obvious periodic oscillation of 0.5–12 m. To reflect this periodic characteristic in the network, the values of former i points are used to obtain the $(i + 1)$th point value. For the component of IMF1, take the anterior six months of data as the network input and present data as the network output. Transform 120 data points of the IMF1 sequence into 114 samples. For the other IMF components and remaining terms, take the data of the anterior 12 months as the network input and the present data as the network output; transform the 120 data points of each sequence into 108 samples.

Determine the Network Training Parameters

Set the RBFNN target error GOAL = 0.0001, spread constant SPREAD = 1, and number of maximum neurons MN = 40.

The Fitting and Forecasting of Model

Train and simulate each RBFNN, and superpose the simulation results. The monthly groundwater depth sequence fitting values of District 6 of Farm Honghe are then obtained (fitting results are shown in Figure 6). The monthly groundwater depth in 2007 is forecasted with the trained network (results shown in Figure 6). From Figure 6, we know that the EMD-RBFNN coupling model of monthly groundwater depth sequence fitting and forecasting in District 6 of Farm Honghe provided better results and almost retained the change trend of the original sequence.

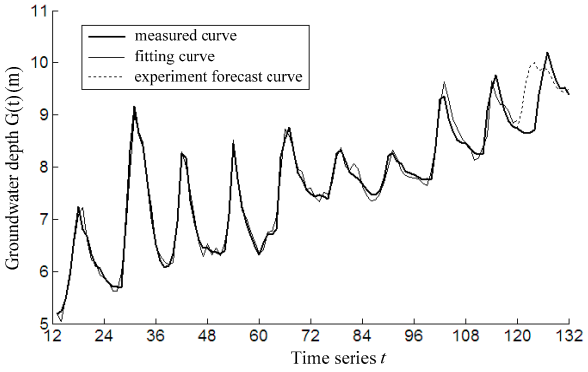

Figure 6. The Fitting and Forecast Curve of Monthly Groundwater Depth Series Forecast Model in District 6 of Farm Honghe (1997–2007).

Testing of Model Accuracy

We use fitting data based on the EMD-RBFNN coupling model to inspect the fitting effect and take the monthly groundwater depth measured data in 2007, which do not include the modelling to inspect the forecasting effect. To test the modelling performance of EMD-RBFNN, the conventional time series model [41] is added. The results are shown in Table 4.

Table 4 shows that the posterior error ratio $C < 0.35$, the small error frequency $p > 0.95$, the relative mean square error $E_1 < 5\%$, the fitting accuracy $E_2 > 0.9$, and the forecasting effect index $E_3 > 80\%$. The checking index has reached level standard I [42]. Meanwhile, compared with the conventional time series model, in fitting stage, the posterior error ratio C represents the mean square error of the fitting residual error sequence per measured data sequence's mean square error. The posterior error ratio C of Conventional Time Series Model is above two times than that of EMD-RBFNN Model; the small error frequency p, the relative mean square error E_1 and the fitting accuracy E_2 are much the same of these two models, especially the fitting accuracy E_2, they're exactly the same. Therefore, these two models have the similar accuracy in this stage. However, in forecasting stage, the forecasting effect index E_3 of the EMD-RBFNN Model is more than that of the Conventional Time Series Model. Namely, the forecasting accuracy of the EMD-RBFNN Model is higher than that of the Conventional Time Series Model, which proves the feasibility and Superiority of the EMD-RBFNN Model. Because the EMD-RBFNN Model can decompose the original monthly groundwater depth sequence whose pattern is complex into IMF component whose pattern is simple and then use the IMF component to build model, which can reduce the error in a large extent, however, the Conventional Time Series Model only use the complex original monthly groundwater depth sequence to build model, which increase the probability of error.

Table 4. Accuracy Test Result of the EMD-RBFNN Coupling Model.

Index		EMD-RBFNN Model	Conventional Time Series Model
Fitting Effect Index	C	0.0871	0.187
	p	1	0.9833
	E_1(%)	4.43	5.14
	E_2	1	1
Experiment Forecast Effect Index	E_3(%)	100	88.89

Therefore, the EMD-RBFNN coupling model of monthly groundwater depth sequence forecasting in District 6 of Farm Honghe provided better results and high accuracy. The model can thus be used to predict the future groundwater depth of District 6 of Farm Honghe.

Groundwater Depth Prediction

The EMD-RBFNN coupling model has been trained well, and the tested accuracy has been used to predict the monthly groundwater depth of District 6 of Farm Honghe in 2008–2011. The prediction value and curve of the groundwater depth are shown in Table 5 and Figure 7, respectively.

Table 5. Groundwater Depth Forecast Value of District 6 in Farm Honghe (2008–2011) (m).

Year	Month												
	1	2	3	4	5	6	7	8	9	10	11	12	Average
2008	9.6280	9.8348	10.0642	10.2046	10.1804	9.9803	9.7434	9.5877	9.4811	9.3986	9.3727	9.4314	9.74
2009	9.5793	9.8101	10.0876	10.3578	10.5288	10.5490	10.4785	10.3633	10.2127	10.0682	9.9639	9.9127	10.16
2010	9.9172	9.9788	10.0949	10.2261	10.2879	10.2115	10.0410	9.8756	9.7603	9.7153	9.7361	9.7410	9.97
2011	9.6692	9.5768	9.5820	9.7411	9.9698	10.1129	10.1029	9.9980	9.8716	9.7503	9.6714	9.6536	9.81

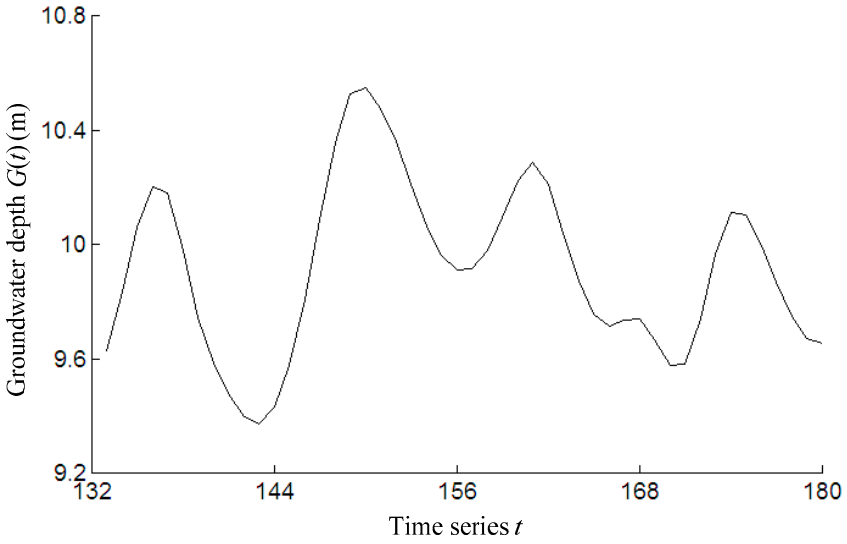

Figure 7. EMD-RBFNN Coupling Model Forecast Curve of Groundwater Depth of District 6 in Farm Honghe (2008–2011).

Table 5 and Figure 7 show that if we continue to apply the current groundwater exploitation practices, the groundwater level of District 6 of Farm Honghe will decrease first and then increase in the future but increase only slightly; the recovery rate of the groundwater will be slow. The annual groundwater depth amplitudes in 2008–2011 were as follows: 0.40 m, 0.42 m, −0.19 m and −0.16 m. The average annual groundwater depth was maintained at approximately 10 m, which shows a large difference of 4–6 m from the ideal groundwater depth. Therefore, the management authorities in District 6 of Farm Honghe should protect limited local groundwater resources.

4.3. Management Countermeasures of Groundwater Resources

Groundwater is a basic resource to support the agricultural production of central Jiansanjiang Administration. Many serious problems such as groundwater table descent are driven by a water usage model that depends on long-term groundwater irrigation. To achieve the sustainable utilization of groundwater resources, this thesis recommends the related local departments take the following management measures:

(1) Speed up the construction of surface water supply infrastructure

Because the surface water control project in central Jiansanjiang Administration is lacking, the proportion of paddy well irrigation is high. Thus, local authorities should complete a field matching project as soon as possible and combine it with local irrigation construction such as Qinlongshan irrigation, 859 irrigation (stage II) and Qianshao irrigation to increase the surface water irrigation area and improve the utilization rate of surface water, thus realizing efficient groundwater resource conservation.

(2) Spread Water-saving Irrigation Technology for Rice

Rice is a conventional crop requiring high water consumption; irrigation water accounts for 95% of the total agricultural water of central Jiansanjiang Administration. Although rice requires a large amount of water, there is considerable water-saving potential. Local authorities should promote irrigation control and adopt other advanced technology to conserve rice irrigation water and promote the development of water-saving agriculture. At present, the conventional net irrigation quota of local rice is approximately 5790 m^3/hm^2 in general, and this value may fall to approximately 4477.6 m^3/hm^2 if the control irrigation technique is used. According to the local hydrological conditions, this could have saved 240 million m^3 of water in 2009. The saved water

could be used to add wetland area or replace the use of groundwater by filling wetlands with saved irrigation water.

(3) Reform the Pricing of Water Use

At present, the agriculture irrigation water price of Heilongjiang Province in China is ¥300/hm^2 in gravity irrigation districts, and it is almost free of charge in well irrigation areas. This type of conventional charging method reduces the water saving consciousness of farmers. Especially in vast well irrigation operations, farmers have been using the free-flooding water method to grow rice, which intensifies the waste of water resources. Thus, local authorities should improve farmers' water saving consciousness through a world water day, China water week and regular lectures on water saving topics, encourage farmers to join water user associations and encourage them to participate in irrigation water management and perfect the water equipment used in irrigation. On this basis, estimating the irrigation water supply will incur a reasonable cost, promote agricultural water price reformation, and implement a method for agricultural water supply according to group usage, thus enabling reasonable agricultural water prices to be set effectively.

5. Conclusions

This paper introduced entropy theory, wavelet theory, fractal theory and other methods to study groundwater depth sequence complexity in the central subarea of Jiansanjiang Administration, and the results are satisfactory.

(1) The complexity of the measurement results shows that the monthly groundwater depth sequence complexity of District 6 of Farm Honghe is the highest. The analysis and prediction results on the situation in District 6 of Farm Honghe can characterize groundwater depth dynamic evolution in the central subarea of Jiansanjiang Administration.

(2) This paper used the EMD method to decompose the monthly groundwater depth sequence of District 6 of Farm Honghe into five IMF sequences and one remainder term. All five IMF sequences have obvious cyclical characteristics. Among these, the sequence variance contribution of IMF2 is the highest, which suggests that the local groundwater depth dynamic changes take one year as the main cycle. The remainder term has obvious linear growth characteristics, which means that the overall pattern of local monthly groundwater depth dynamic change is a gradual increase. The RBFNN is used to fit and forecast series of EMD decomposition, and the accuracy testing results show the high robustness of the EMD-RBFNN coupling model. The prediction results of this model show that the local groundwater depth will remain at a 10 m level if we continue to use the current agricultural water use model that depends on groundwater. Therefore, increasing the proportion of surface water irrigation, extending water-saving irrigation techniques in paddy rice, carrying out agricultural water price reform and other methods will become important measures to restore local groundwater levels.

(3) The selection of the boundary extension and calibration of the spread constant and the largest neuron number are the key scientific problems in the application of EMD and RBFNN. The different boundary extension measures can lead to different results and operational efficiency results of the EMD, and the different network training parameters may influence the fitting and forecast accuracy of the RBFNN. Therefore, the focus on the different hydrological time series will become an important hydrological research direction to forecast how to choose a reasonable boundary extension plan to solve the end effect of EMD and how to determine training parameters to improve the operational efficiency and extension effect of the RBFNN.

Acknowledgments: This study has been financially supported by the National Natural Science Foundation of China (Grants 51479032, 51279031, 51579044), Yangtze River Scholars in Universities of Heilongjiang Province, Water Conservancy Science and Technology Project of Heilongjiang Province (Grants 201318, 201503), the Outstanding Youth Fund of Heilongjiang Province (Grants JC201402), and the Humanity and Social Science Youth Foundation of Ministry of Education of China (Grants 14YJCZH017).

Author Contributions: Qiang Fu and Dong Liu designed the study. Qiang Fu wrote the manuscript. Tianxiao Li and Song Cui performed data analysis. Tianxiao Li and Yuxiang Hu reviewed and approved the manuscript.

Conflicts of Interest: The authors declare no conflict of interest.

References

1. Li, Z.W. Temporal Scaling and Complexity Analyses of Dynamic Groundwater Systems. Ph.D. Thesis, The University of Iowa, Iowa City, IA, USA, 2006.
2. Cantone, J.; Schmidt, A. Improved understanding and prediction of the hydrologic response of highly urbanized catchments through development of the Illinois Urban Hydrologic Model. *Water Resour. Res.* **2011**, *47*, 427–438. [CrossRef]
3. Březková, L.; Šálek, M.; Soukalová, E.; Starý, M. Predictability of Flood Events in View of Current Meteorology and Hydrology in the Conditions of the Czech Republic. *Soil Water Res.* **2007**, *2*, 156–168.
4. Daliakopoulosa, I.N.; Coulibalya, P.; Tsanis, I.K. Groundwater level forecasting using artificial neural networks. *J. Hydrol.* **2005**, *309*, 229–240. [CrossRef]
5. Adamowski, J.; Chan, H.F. A wavelet neural network conjunction model for groundwater level forecasting. *J. Hydrol.* **2011**, *407*, 28–40. [CrossRef]
6. Affandi, A.K.; Watanabe, K. Daily groundwater level fluctuation forecasting using soft computing technique. *Nat. Sci.* **2007**, *5*, 1–10.
7. Lin, G.F.; Chen, L.H. Time series forecasting by combining the radial basis function network and the self-organizing map. *Hydrol. Process.* **2005**, *19*, 1925–1937. [CrossRef]
8. Dash, N.B.; Panda, S.N.; Remesan, R.; Sahoo, N. Hybrid neural modeling for groundwater level prediction. *Neural Comput. Appl.* **2010**, *19*, 1251–1263. [CrossRef]
9. Bidwell, V.J. Realistic forecasting of groundwater level, based on the eigen structure of aquifer dynamics. *Math. Comput. Simul.* **2005**, *69*, 12–20. [CrossRef]
10. Hong, Y.M.; Wan, S. Forecasting groundwater level fluctuations for rainfall-induced landslide. *Nat. Hazards* **2011**, *57*, 167–184. [CrossRef]
11. Izady, A.; Davary, K.; Alizadeh, A.; Ghahraman, B.; Sadeghi, M.; Moghaddamnia, A. Application of "panel-data" modeling to predict groundwater levels in the Neishaboor Plain, Iran. *Hydrogeol. J.* **2011**, *20*, 435–447. [CrossRef]
12. Chebud, Y.; Melesse, A. Operational Prediction of Groundwater Fluctuation in South Florida Using Sequence Based Markovian Stochastic Model. *Water Resour. Manag.* **2011**, *25*, 2279–2294. [CrossRef]
13. He, B.; Takase, K.; Wang, Y. Regional groundwater prediction model using automatic parameter calibration SCE method for a coastal plain of Seto Inland Sea. *Water Resour. Manag.* **2007**, *21*, 947–959. [CrossRef]
14. Huang, N.E.; Shen, Z.; Long, S.R.; Wu, M.C.; Shih, H.H.; Zheng, Q.; Yen, N.-C.; Tung, C.C.; Liu, H.H. The empirical mode decomposition and the Hilbert spectrum for nonlinear and non-stationary time series analysis. *Proc. R. Soc. Lond. A Math. Phys. Eng. Sci.* **1998**, *454*, 903–995. [CrossRef]
15. Blanco-Velasco, M.; Weng, B.; Barner, K.E. ECG signal denoising and baseline wander correction based on the empirical mode decomposition. *Comput. Biol. Med.* **2008**, *38*, 1–13. [CrossRef] [PubMed]
16. Guhathakurta, K.; Mukherjee, I.; Chowdhury, A.R. Empirical mode decomposition analysis of two different financial time series and their comparison. *Chaos Solitons Fractals* **2008**, *37*, 1214–1227. [CrossRef]
17. Coughlin, K.T.; Tung, K.K. 11-Year solar cycle in the stratosphere extracted by the empirical mode decomposition method. *Adv. Space Res.* **2004**, *34*, 323–329. [CrossRef]
18. Bassiuny, A.M.; Li, X.; Du, R. Fault diagnosis of stamping process based on empirical mode decomposition and learning vector quantization. *Int. J. Mach. Tools Manuf.* **2007**, *47*, 2298–2306. [CrossRef]
19. Sinclair, S.; Pegram, G.G.S. Empirical Mode Decomposition in 2-D space and time: A tool for space-time rainfall analysis and nowcasting. *Hydrol. Earth Syst. Sci.* **2005**, *9*, 127–137. [CrossRef]
20. Iyengar, R.N.; Kanth, S.T.G.R. Intrinsic mode functions and a strategy for forecasting Indian monsoon rainfall. *Meteorol. Atmos. Phys.* **2005**, *90*, 17–36. [CrossRef]
21. Huang, Y.; Schmitt, F.G.; Lu, Z.; Liu, Y. Analysis of daily river flow fluctuations using empirical mode decomposition and arbitrary order Hilbert spectral analysis. *J. Hydrol.* **2009**, *373*, 103–111. [CrossRef]
22. Mcmahon, T.A.; Vogel, R.M.; Peel, M.C.; Pegram, G.G.S. Global streamflows—Part 1: Characteristics of annual streamflows. *J. Hydrol.* **2007**, *347*, 243–259. [CrossRef]
23. Lin, G.F.; Chen, L.H. A non-linear rainfall-runoff model using radial basis function network. *J. Hydrol.* **2004**, *289*, 1–8. [CrossRef]

24. Chen, H.; Kim, A.S. Prediction of permeate flux decline in crossflow membrane filtration of colloidal suspension: A radial basis function neural network approach. *Desalination* **2006**, *192*, 415–428. [CrossRef]
25. Liu, D.; Zhou, M.; Meng, J. Application of Approximate Entropy for Analyzing Complexity of Groundwater Depth Series in Sanjiang Plain. *J. Nat. Resour.* **2012**, *27*, 115–121. (In Chinese)
26. He, Z.; Gao, S.; Chen, X.; Zhang, J.; Bo, Z.; Qian, Q. Study of a new method for power system transients classification based on wavelet entropy and neural network. *Int. J. Electr. Power Energy Syst.* **2011**, *33*, 402–410.
27. Pincus, S.M. Approximate entropy as a measure of system complexity. *Proc. Natl. Acad. Sci. USA* **1991**, *88*, 2297–2301. [CrossRef] [PubMed]
28. Zhao, H.; Wang, G.; Xu, C.; Yu, F. Voice Activity Detection Method Based on Multivalued Coarse-Graining Lempel-Ziv Complexity. *Comput. Sci. Inf. Syst.* **2011**, *8*, 869–888. [CrossRef]
29. Duarte, M.; Zatsiorsky, V.M. On the fractal properties of natural human standing. *Neurosci. Lett.* **2000**, *283*, 173–176. [CrossRef]
30. Planinšič, P.; Petek, A. Characterization of corrosion processes by current noise wavelet-based fractal and correlation analysis. *Electrochim. Acta* **2008**, *53*, 5206–5214. [CrossRef]
31. Wang, W.S.; Xiang, H.L.; Huang, W.J.; Ding, J. Study on fractal dimension of runoff sequence based on successive wavelet transform. *J. Hydraul. Eng.* **2005**, *36*, 598–601.
32. Wu, F.; Qu, L. An improved method for restraining the end effect in empirical mode decomposition and its applications to the fault diagnosis of large rotating machinery. *J. Sound Vib.* **2008**, *314*, 586–602. [CrossRef]
33. Peel, M.C.; Amirthanathan, G.E.; Pegram, G.G.S.; McMahon, T.A.; Chiew, F.H.S. Issues with the Application of Empirical Mode Decomposition Analysis. In Proceedings of the International Congress on Modelling and Simulation, Melbourne, Australia, 12–15 December 2005; pp. 1681–1687.
34. Su, Y.; Liu, Z.; Li, K.; Huo, B. A new method for end effect of EMD and its application to harmonic analysis. *Adv. Technol. Electr. Eng. Energy* **2008**, *27*, 33–37.
35. Parey, A.; Pachori, R.B. Variable cosine windowing of intrinsic mode functions: Application to gear fault diagnosis. *Measurement* **2012**, *45*, 415–426. [CrossRef]
36. Yang, Z.; Yang, L.; Qing, C. An oblique-extrema-based approach for empirical mode decomposition. *Digit Signal Process.* **2010**, *20*, 699–714. [CrossRef]
37. Lu, W.C.; Xue, H.; Liu, C.W.; Gao, N. Study of forecasting model of customer retention for supermarket based on RBF neural network. *J. Beijing Technol. Bus. Univ. Nat. Sci. Ed.* **2009**, *27*, 45–48. (In Chinese)
38. Moradkhani, H.; Hsu, K.L.; Gupta, H.V.; Sorooshian, S. Improved stream flow forecasting using self-organizing radial basis function artificial neural networks. *J. Hydrol.* **2004**, *295*, 246–262. [CrossRef]
39. Rakhshandehroo, G.R.; Shaghaghian, M.R.; Keshavarzi, A.R.; Talebbeydokhti, N. Temporal variation of velocity components in a turbulent open channel flow: Identification of fractal dimensions. *Appl. Math. Model.* **2009**, *33*, 3815–3824. [CrossRef]
40. Klionsky, D.M.; Oreshko, N.I.; Geppener, V.V. Empirical Mode Decomposition in Segmentation and Clustering of Slowly and Fast Changing Non-Stationary Signals. *Pattern Recognit. Image Anal.* **2009**, *19*, 14–29. [CrossRef]
41. Erdoğan, H.; Gülal, E. The application of time series analysis to describe the dynamic movements of suspension bridges. *Nonlinear Anal. Real World Appl.* **2009**, *10*, 910–927. [CrossRef]
42. Luan, Z.Q.; Liu, G.H.; Yan, B.X. Application of Time-Series Model to Predict Groundwater Dynamic in Sanjiang Plain, Northeast China. *Wetl. Sci.* **2011**, *9*, 47–51. (In Chinese)